https://doi.org/10.5194/egusphere-2026-547
Preprint. Discussion started: 11 February 2026

ENSO teleconnections in eddy-rich climate models

Bianca Mezzina[1], Christopher David Roberts[1], Matthias Aengenheyster[1], Rohit Ghosh[2], Malcolm John Roberts[3], Marc Batlle Martin[4]

[1]European Centre for Medium Range Weather Forecasts (ECMWF), Reading, UK & Bonn, Germany
[2]Alfred Wegener Institute Helmholtz Centre for Polar and Marine Research, Bremerhaven, Germany
[3]Met Office Hadley Centre, Exeter, UK
[4]Barcelona Supercomputing Center, Barcelona, Spain

Correspondence to: Bianca Mezzina (bianca.mezzina@ecmwf.int)

Abstract. We examine how ENSO atmospheric teleconnections are represented in a novel suite of coupled simulations with eddy-resolving ocean and high-resolution atmosphere, at an unprecedented grid spacing of ~10 km in both components. The single-member, multi-decadal experiments have been performed under a coordinated protocol within the European Eddy-RIch Earth System Models (EERIE) project using three different models.

To assess the performance of the EERIE models, we design tailored metrics to encapsulate and quantify different aspects of the ENSO teleconnections: direct tropical response, Rossby wave sources, extra-tropical tropospheric and stratospheric anomalies, and surface impacts. The metrics are based on linear regressions on the Niño3.4 index of several atmospheric fields in early- and late winter. Additionally, we apply the same diagnostics to a set of complementary atmosphere-only simulations run at lower resolution (~30 km, 10 members) and high resolution (~10 km, 1 member), which allow to isolate the impact of atmospheric resolution and estimate the internal variability.

We find mixed results in the EERIE coupled simulations compared to previous generation eddy-parametrized and eddy-permitting models (maximum ~25 km in both atmosphere and ocean). The performance, though overall positive, varies by season, region, and model configuration and a systematic improvement does not emerge clearly. Similarly, the atmosphere-only experiments also indicate limited advances from the increased atmospheric resolution. However, potential benefits may be hindered by the large uncertainty in the ENSO response due to internal variability and sampling.

https://doi.org/10.5194/egusphere-2026-547
Preprint. Discussion started: 11 February 2026

1 Introduction

Increasing the horizontal resolution of Earth system models has proven beneficial for the representation of different climate processes (Roberts M. et al., 2018; Docquier et al. 2019; Liu X. et al. 2021, Athanasiadis et al., 2022, Yeager et al., 2023). A significant advance in model fidelity may be achieved by explicitly resolving mesoscale ocean processes, such as eddies and boundary currents, which are crucial for the transport of energy and mass (Bryan et al., 2007, Hewitt et al. 2020; see Dong et al. 2025 for a review). However, current climate models feature a variety of ocean regimes with limited representation of these dynamics. Full parametrization of the mesoscale eddies is required for an ocean resolution coarser than 1°, as in most models contributing to the Coupled Model Intercomparison Project Phase 6 (CMIP6). In contrast, "eddy-permitting" models (~0.25°) can partially represent mesoscale eddies and typically resolve them at lower latitudes. This is the case of some operational forecasting systems (e.g. ECMWF's SEAS5; Johnson et al., 2019), as well as models contributing to the High Resolution Model Intercomparison Project (HighResMIP). Finally, only a minority of models are "eddy-rich" (or "eddy-resolving"): with a resolution of ~0.1°, they can resolve mesoscale eddies over most of the mid latitudes, though not fully in coastal regions (Hallberg, 2013).

Previous studies have shown the benefits of resolving eddies for ocean biases and documented the effect of coupling with a coarser atmosphere (e.g. Hewitt et al., 2020), but little is known about the impact of eddy-rich oceans with an atmosphere of comparable resolution. Even less when it comes to long (e.g. multi-decadal) simulations, which are needed to assess the potential role of the ocean mesoscale on climate (e.g. Rackow et al., 2022). To address this, the European Eddy-RIch Earth System Models (EERIE) project has successfully completed a novel set of coupled simulations with eddy-resolving ocean and high-resolution atmosphere (~10 km in both) over the period 1950-2014. These experiments, run with different models under coordinated, standard protocols, constitute a unique ensemble to assess and quantify the impact of these unprecedented resolutions on the climate system.

The El Niño-Southern Oscillation (ENSO) is a prominent mode of climate variability that can impact remote regions through atmospheric teleconnections, whose simulation remains a challenge (see Taschetto et al., 2020 for a review). Though the mechanisms for a possible direct impact of the ocean mesoscale are still debated, there are serval ways through which a better resolved ocean could affect these teleconnections. Various studies have shown that higher ocean resolution can improve known biases in Tropical Pacific sea surface temperature (SST) and the representation of ENSO patterns (e.g. Liu B. et al., 2022). This can, in turn, positively impact the local response to ENSO, such as deep convection and precipitation in the Tropical Pacific (e.g. Williams et al., 2024). A consequent effect on the extra-tropical teleconnection is possible, since the tropical atmospheric response triggers a poleward-propagating Rossby wave train. Besides, the ocean resolution can also modify the atmospheric basic state, which further influences the wave train generation and propagation (e.g. Dawson et al., 2011). Some encouraging results in this direction were presented by Dawson et al. (2013), who found a more realistic extra-tropical response

https://doi.org/10.5194/egusphere-2026-547
Preprint. Discussion started: 11 February 2026

to ENSO when the ocean resolution was increased to 1/3° in the coupled model HiGEM, independent of the atmosphere. More recently, Williams et al. (2024) analysed a large set of models from HighResMIP and found that high-resolution configurations show a more accurate representation of the position of the North Pacific response in the multi-model mean, especially during El Niño, and attributed these differences to the increased ocean resolution. However, they detected no significant improvement in the strength of the teleconnection. Similar conclusions were drawn by Fang et al. (2024) for the teleconnection in the Southern Hemisphere.

Atmospheric resolution can also play a role. Roberts C. et al. (2018), using an ensemble based on the ECMWF's Integrated Forecasting System (IFS), found more accurate late-winter ENSO teleconnections in the North Atlantic when the atmospheric resolution was enhanced. Molteni et al. (2020) confirmed these results but also concluded that no systematic impact from finer atmospheric resolutions was evident in a multi-model ensemble from HighResMIP. Similarly, Dawson et al. (2013) deduced that increasing the atmospheric resolution alone has no significant impact on the extra-tropical teleconnection.

The impact of high resolution on ENSO teleconnections is thus unclear, and no assessment has been carried out so far using climate simulations at the 10-km scale employed in EERIE. The goal of this study is precisely to evaluate the representation of ENSO teleconnections in these novel eddy-rich models and determine whether any systematic improvement can be detected, with respect to previous generation state-of-the-art models.

To this end, we rely on the current knowledge of the driving mechanisms of the teleconnections and try to examine step-by-step the chain of processes from the tropics to the mid latitudes. First, we assess the atmospheric response in the ENSO region. The anomalous SST alter the low-level circulation, causing rising motions in the central Tropical Pacific and compensating divergent flow in the upper troposphere (in the case of El Niño). These changes are balanced by the opposite response in the western and eastern Tropical Pacific (e.g. García-Serrano et al., 2017). Diagnosing these anomalies in the upper troposphere is crucial, since they act as the main trigger for the extra-tropical Rossby wave train (e.g. Trenberth et al., 1998). Our next step is then to examine anomalies in the Rossby Wave Source (RWS), which highlight the actual regions favouring (or suppressing) the generation of Rossby waves (Sardeshmukh and Hoskins, 1988). For ENSO, these regions are mainly located in the Pacific, but some secondary sources over the Atlantic have also been indicated as potential contributors to the North Atlantic response (Toniazzo and Scaife, 2006; Hardiman et al., 2019). Next, we focus on the Rossby wave train, which represents the main driver of the extra-tropical teleconnection. The wave train consists of alternating anomalous highs and lows in the North Pacific, North America and North Atlantic, but this response is only established in late winter, from January onwards (e.g. Bladé et al., 2008). The anomalies extend to the surface with a slight vertical tilt and produce a dipolar pattern in the North Atlantic that resembles the negative phase of the North Atlantic Oscillation (NAO; e.g. Mezzina et al., 2020). In contrast, the early-winter signal does not show clear centres of action in the North Pacific and North America, while a positive NAO-like dipole dominates the North Atlantic, especially at surface (e.g. Ayarzagüena et al., 2018). Impacts from the Indian Ocean, the Caribbean Sea and other basins have been suggested to influence this signal, which is still not fully understood (Ayarzagüena et al., 2018; Abid et al., 2021; Molteni and Brookshaw, 2023). We also evaluate the impact of ENSO on the stratospheric polar vortex, another potential contributor to the North Atlantic surface signal in late winter. The stratospheric

https://doi.org/10.5194/egusphere-2026-547
Preprint. Discussion started: 11 February 2026

response mainly consists in a deceleration of the vortex and warming of the lower polar stratosphere (for El Niño; see Domaisen et al., 2019 for a review). For each of these aspects, we design a related metric to encapsulate and quantify the response in a single value, which we can use to benchmark the performance of the EERIE simulations with respect to other models.

A prominent, long-standing issue of ENSO teleconnections is related to how the atmospheric internal variability can modulate or mask the forced signal (e.g. Deser et al., 2017). The EERIE coupled simulations consist of a single realization for each model, so it is not possible to fully disentangle the forced and noisy components, despite the relatively large number of simulated years. However, an additional set of simulations performed within EERIE can help with this issue. Atmosphere-only experiments with prescribed SST from observations have been run using IFS. An ensemble of 10 members is available for a low-resolution configuration, together with a corresponding single member with 10-km resolution, as in the coupled experiments. In this set up, it is possible to quantify potential differences in the ENSO response arising from the different atmospheric resolution and to place them in the context of internal variability, namely comparing them to the ensemble spread. Additionally, since some coupled simulations share this same atmospheric component (see Methods), we can also evaluate the impact of prescribed SST versus an interactive ocean.

The EERIE models and experiments, together with the other data and methods used, are described in detail in Sect. 2. The coupled runs are then examined in Sect. 3, while the main results from the atmosphere-only simulations are reported in Sect. 4. The findings are summarized and discussed in Sect. 5.

2 Data and Methods

2.1 EERIE models and experiments

2.1.1 Coupled simulations

We examine coupled simulation from three eddy-rich climate models contributing to the EERIE Phase 1 simulations (Roberts M. et al., 2024). The models, with the short names used in this paper, are:

- IFS-FESOM, a recent coupled set-up between IFS and the Finite VolumE Sea ice-Ocean Model (FESOM). IFS is run in a climate configuration based on Cylce 48r1, with atmospheric horizontal resolution of ~10 km (Tco1279) and 137 vertical levels. The standard operational settings for the deep convection scheme are maintained. FESOM (version 2.5) uses an NG5 grid that provides a horizontal resolution between 5 and 13 km (Rackow et al., 2024).
- IFS-NEMO, where the same configuration of IFS is coupled to the ocean model NEMO (version 4.0.7; Madec et al., 2019) combined with the sea ice model SI3 (Vancoppenolle et al., 2023). The ocean grid is eORCA12, corresponding to a resolution of ~8 km.

https://doi.org/10.5194/egusphere-2026-547
Preprint. Discussion started: 11 February 2026

- HadGEM, based on a modified configuration of the UK Met Office Global Coupled Model (version GC5). The atmospheric component is the Met Office Unified Model with horizontal resolution ~20-30 km (N640). It includes a new convection parameterisation scheme, CoMorphA (Lock et al., 2024). The ocean model is NEMO (version 4.04), again using eORCA12, with SI3 as sea ice component (Blockley et al., 2024) and with a configuration based on GOSI9 (Guiavarc'h et al., 2025).

Hence, our models include two with the same atmosphere (IFS), and two with very similar ocean components (NEMO eORCA12).

The experiments are single-member, multi-decadal simulations conducted under established protocols. For IFS-FESOM and IFS-NEMO, a protocol similar to HighResMIP (Haarsma et al., 2016) is followed to produce historical simulations spanning 1950-2014. For HadGEM, the CMIP6 DECK approach is used, with the simulation starting in 1850. However, in this paper we only examine the common period 1950-2014 for all three models, which we will refer to as "EERIE coupled".

Further details on the simulations and their validation can be found in Roberts M. et al. (2024). This paper focuses on the atmospheric teleconnections and a detailed evaluation of ENSO itself is beyond our scope. We simply report that the ENSO cycle in the EERIE models is overall realistic and comparable to other state-of-the-art coupled models, despite some deficiencies such as the dampened cycle in IFS-NEMO and the stronger variability in IFS-FESOM and HadGEM (Fig. S1).

2.1.2 Atmosphere-only simulations

In addition to the coupled simulations, we also analyse atmosphere-only experiments (EERIE AMIP for brevity) performed with two configurations of the IFS atmospheric model: ten "low resolution" (IFS-LR) members, with horizontal grid spacing of ~28 km, and one "high resolution" (IFS-HR) member, with horizontal grid spacing of ~9 km. In these simulations, the model is not coupled to an ocean-sea ice component but is instead forced by time-evolving SST and sea ice concentration from observations. The period covered is 1980 to 2023, and the IFS version is the same used in the coupled runs (IFS-NEMO and IFS-FESOM). A detailed description and validation can be found in Aengenheyster et al. (2025).

2.2 Other Data and Methods

Throughout our analysis, we systematically compare the model's results to ERA5 (Hersbach et al., 2020). The main period of reference is 1950-2014, which we refer to as ERA5-hist in Sect. 3.5, and as ERA5 in the rest. In Sect. 3.5, we also use the period 1980-2023 (labelled ERA5-rec) as baseline for the EERIE AMIP runs. Though this is a reanalysis product, in this context it represents the best estimate for the "real world" and thus we use "observations" and "reanalysis" interchangeably.

Besides comparing the EERIE models with reanalysis, we also benchmark them against a subset of simulations from HighResMIP, namely the ones used in Molteni et al. (2020; see Table S1). The selection consists of 6+6 models, with corresponding "low" and "high" resolution versions (LR and HR for brevity). The atmospheric resolution is 50-250 km for LR and 25-100 km for HR, while the ocean is 25-100 km for LR ("eddy-parametrized") and 25-50 km for HR ("eddy-

https://doi.org/10.5194/egusphere-2026-547
Preprint. Discussion started: 11 February 2026

permitting"; see Table S1 for more details). For each model, we analyze two types of experiments: coupled simulations analogous to the EERIE coupled runs ("hist-1950") and forced-atmosphere experiments similar to the EERIE AMIP ones, but over the period 1950-2014 ("highresSST-present"). A varying number of members is available for each model and experiment, for a total of 31 for the coupled simulations and 29 for the AMIPs (Table S1; note that less members were used in Molteni et al., 2020). Due to data issues, the models from CNRM-CERFACS are excluded from the analysis of the 200-hPa geopotential height (Sect. 3.3).

We define the Niño3.4 (N3.4) index using the standardized, detrended time series of SST anomalies in the Niño3.4 region (5°N-5°S, 120°W-170°W) in December-February (DJF). All the metrics used to assess the ENSO response, whose details are reported in the respective sections, are based on linear regressions of atmospheric fields, which are also previously detrended. The regressions represent the response to a change in one standard deviation of the N3.4 index. Two seasons are mainly considered: early winter (November-December) and late winter (January-February). Note that for both seasons we use the same DJF-based N3.4 index instead of ND- and JF- based ones, given their extremely high correlations (Fig. S2). Statistical significance is assessed with Student's t-test at the 95% confidence level.

In Section 3.5, we discuss Taylor diagrams (Taylor, 2001) for the anomalous sea-level pressure (SLP) patterns in the North Atlantic-European (NAE) sector, with boundaries at 20°N, 90°N and 90°W, 40°E. In these plots, two values are depicted: (i) the correlation between the spatial patterns in ERA5 and the models as the angle, and (ii) the ratio between the standard deviations in the models and ERA5 as the radial distance from the origin. By definition, ERA5 has thus correlation and standard deviation ratio equal to 1. An additional property of these plots is that the centered root-mean-square error is proportional to the distance from ERA5, though this is not marked in our plots. To build these plots, the SLP has been regridded to a common 1°x1° grid, which is suitable to evaluate these types of large-scale patterns.

As mentioned above, one of our targets is to benchmark the EERIE models against HighResMIP, for which we define tailored metrics to encapsulate the responses. However, we are not only interested in evaluating the performances in the single metrics, but also in determining if there is any systematic improvement. To this end, we associate a "ranking" to each metric. We order the 31 HighResMIP coupled members and the 3 EERIE models (34 simulations in total) based on the error, defined as the absolute difference with respect to ERA5. For some metrics, this only implies differences in the amplitude, while for others there are two rankings based on the amplitude and the longitude, separately. We can thus determine, for each case, whether the EERIE models perform: (i) "better" than most HighResMIP members (ranking n. 1 to 11), (ii) "average" (n. 12 to 22) or (iii) "worse" (n. 23 to 34). The main values for the EERIE models are reported in the text, while the rest can be found in Fig. 10, which acts as a summary.

https://doi.org/10.5194/egusphere-2026-547
Preprint. Discussion started: 11 February 2026

2.3 Tropical Rossby Wave Source

The RWS is a common diagnostic used to identify regions favouring the generation of Rossby waves. Here, we focus on one specific component of the RWS, the so-called "tropical" part (TRWS):

$$TRWS = -\boldsymbol{V}'_{\chi} \cdot \boldsymbol{\nabla}(\bar{\zeta} + f)$$

Where $\boldsymbol{V}'_{\chi}$ is the anomalous divergent wind, $\bar{\zeta}$ is the climatological vorticity and f is the Coriolis parameter. This term emerges after linearizing the advective component of the RWS and discarding the advection of anomalous vorticity by the climatological divergent wind, which is negligible (Qin and Robinson, 1993). The TRWS has been used in previous ENSO studies (e.g. Mezzina et al., 2022; Sabatani et al., 2025) and represents a pure source that is suggested to be the main trigger for extra-tropical teleconnections (Qin and Robinson, 1993). In contrast, we do not consider the "extra-tropical" component, where the source and response are entangled. Sabatani et al. (2025) also considered the TRWS but confirmed that their conclusions remain valid when both components are included. On top of presenting regression maps of the TRWS, we also evaluate regressions of their averages over four different regions: Western Pacific (20-40°N, 80-140°E), Tropical Pacific (0-30°N, 180-120°W), Tropical Atlantic (5-25°N, 70-2-°W), Western Atlantic (25-45°N,110-60°W). These regions are based on the definitions of Sabatani et al. (2025), though with different names. To ease the computation, the TRWS is computed with T20 truncation, which is sufficient for planetary waves.

https://doi.org/10.5194/egusphere-2026-547
Preprint. Discussion started: 11 February 2026

3 Results from the coupled simulations

3.1 Tropical response

Our first step is to assess the local atmospheric response to ENSO. Specifically, changes in the upper-tropospheric divergence in the Tropical Pacific are expected. To evaluate this response in the EERIE models and compare it to ERA5, we first examine regressions maps of early-winter 200-hPa velocity potential anomalies on the N3.4 index (Fig. 1, contours). All three models capture the anomalous upper-level divergent flow in the central Tropical Pacific (negative anomalies) and the accompanying convergence over the Maritime continent (positive anomalies). However, differences in the pattern and amplitude of the response are present, likely resulting from distinct SST anomalies associated to each model's specific ENSO.

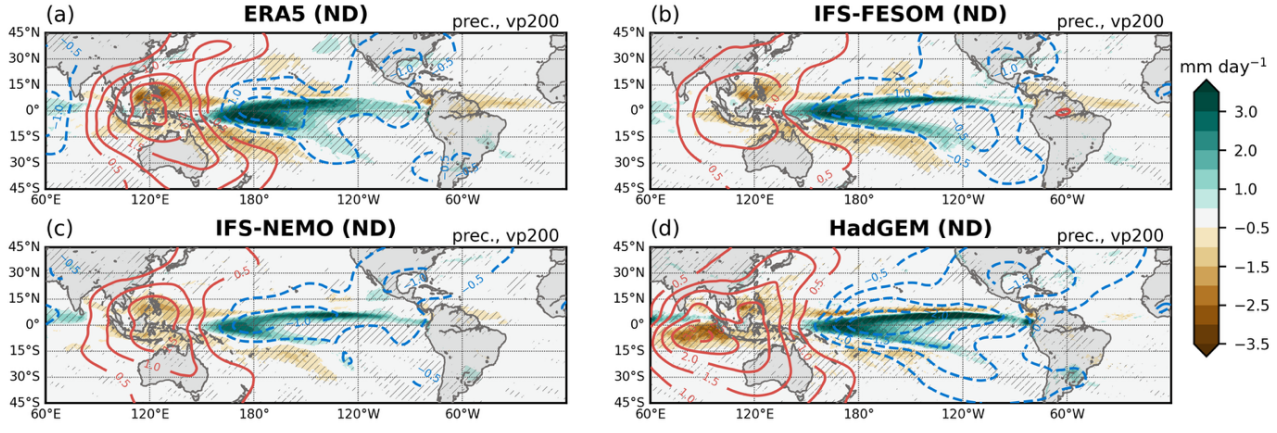

Figure 1: Linear regression on the N3.4 index of precipitation (shadings) and 200-hPa velocity potential (contours) anomalies in Nov-Dec for (a) ERA5 and (b-d) the EERIE coupled models. Hatches indicate statistical significance at the 95% level for the precipitation. Only significant values of the velocity potential are shown. Contour interval: 0.5x10^6 m^2 s^{-1}.

The negative anomalies in the central Tropical Pacific represent the upper-tropospheric divergence linked to the rising motions that are a direct response to ENSO. In principle, it is crucial that this aspect is well simulated for the extra-tropical Rossby wave train to be properly generated. To further detect the differences and better evaluate the performance of the EERIE models, we define our first tailored metric. First, we carry out a similar regression, but using the 200-hPa velocity potential averaged over the over the latitudinal band between 15°N and 15°S. Given the rough symmetry of the spatial patterns across the equator (Fig. 1), this is a suitable, simple diagnostic that encapsulates the response and allows for an easier comparison between the EERIE models, ERA5 and HighResMIP (Fig. S3). Next, we detect the location of the minimum in these regressions – corresponding to the anomalies in the central Tropical Pacific – measure the related amplitude, and show these values together in a scatterplot (Fig. 2a). Overall, all models tend to either show a too weak, too west response compared to ERA5 (like IFS-

https://doi.org/10.5194/egusphere-2026-547
Preprint. Discussion started: 11 February 2026

NEMO and IFS-FESOM), or one that is too strong and displaced eastward (like HadGEM). While the EERIE models are generally within the range of HighResMIP, they perform especially poorly in terms of amplitude. When ranking the simulations according to the amplitude error (see Methods), they are among the worst models (Fig. 10, 1st column).

We can repeat the analysis using precipitation anomalies, which also indicate areas of vertical motions, thought they are more spatially heterogenous (Fig. 1, shading). In this case, the scatter plot describing the location and amplitude of the precipitation peak in the central Tropical Pacific – computed in a similar way – suggests that in most members the response is too weak and too west (Fig. 2c), and confirms the rather poor performance of the EERIE models, which are again worse than most HighResMIP members (see also Fig. 10, 2nd column).

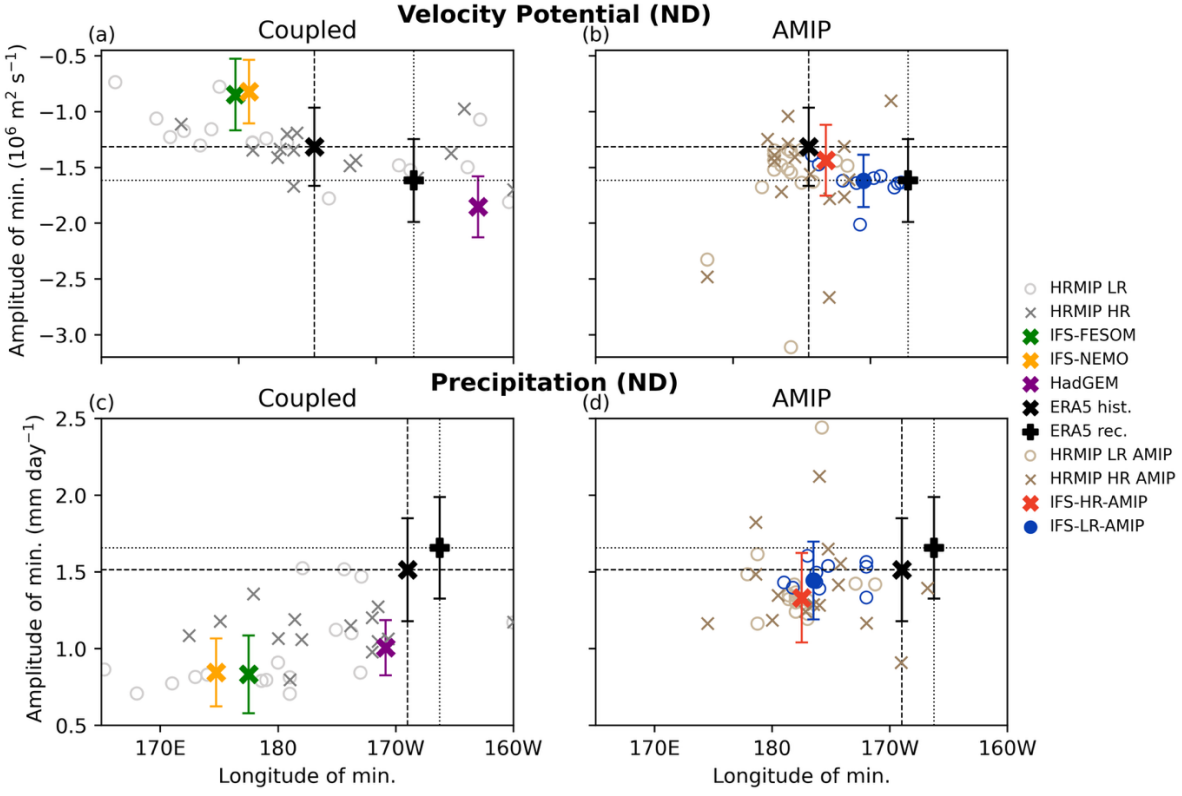

Figure 2: Top: Longitude and amplitude of the minimum in the 200-hPa velocity potential anomalies averaged between 15°N and 15°S and regressed on the N3.4 index, in Nov-Dec. Bottom: same, but for the maximum precipitation. Left: Coupled runs. Right: AMIP runs. ERA5 hist. =1950-2014, ERA5 rec.= 1980-2023. The empty blue circles indicate the single members form the EERIE IFS-LR ensemble, with the filled circle represent the ensemble mean. The vertical bars indicate the confidence interval at the 95% level.

https://doi.org/10.5194/egusphere-2026-547
Preprint. Discussion started: 11 February 2026

3.2 TRWS

While the direct upper-tropospheric response in the ENSO region constitutes the first trigger for the extra-tropical Rossby train, the full description of its generation is more complex, as the interaction between divergence and vorticity needs to be considered. Here, we examine how the tropical component (TRWS), which describes the advection of climatological absolute vorticity by the anomalous divergent wind (see Methods), is captured in the EERIE models (Fig. 3). The west-east dipole of anomalous convergence-divergence in the western and central Tropical Pacific is related to the TRWS anomalies of opposite sign over eastern Asia (positive TRWS) and around the date line (negative TRWS). These are both well captured by the EERIE models, though with varying amplitudes and patterns. In contrast, the models seem to struggle in other regions with secondary sources, such as the North Atlantic, where they mostly tend to overestimate the response.

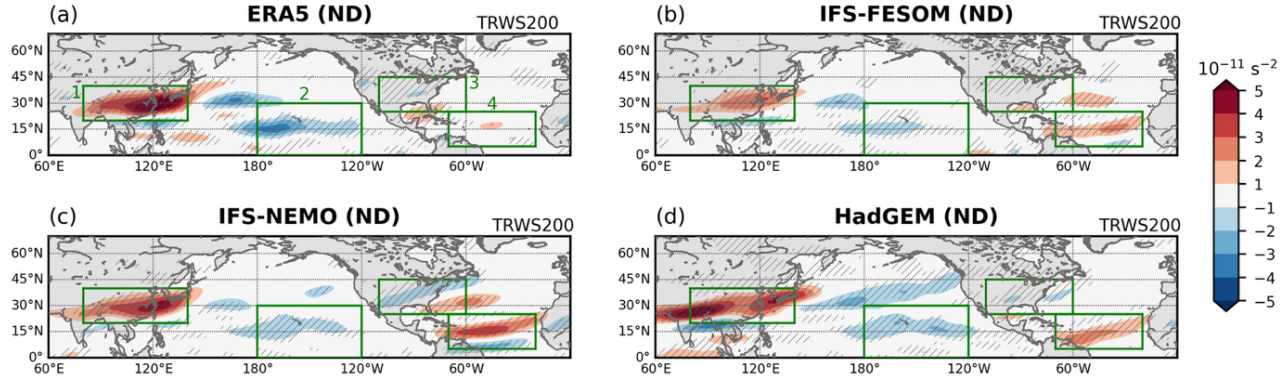

Figure 3: Linear regression on the N3.4 index of 200-hPa TRWS anomalies in Nov-Dec for (a) ERA5 and (b-d) the EERIE coupled models. Hatches indicate statistical significance at the 95% level. The green boxes show the regions used to compute the averages shown in Figure 4: 1=Western Pacific; 2=Tropical Pacific; 3=Western Atlantic; 4=Tropical Atlantic. See main text for details on the computation of the TRWS.

To quantify this response, we design four metrics based on the linear regression of the TRWS averaged over the regions highlighted in Fig. 3 (and defined in the Methods). In the Tropical Pacific (Fig. 4b), the observed response is well within the range of the simulations. While the EERIE models do not stand out from the group, they perform surprisingly well considering their poor representation of the tropical response (IFS-NEMO ranks n. 13, HadGEM n. 5 and IFS-FESOM n. 23). Similarly, IFS-NEMO and HadGEM are again among the best 10 models in the Western Pacific, where the response is typically too weak (Fig. 4b, Fig. 10, 3rd column). The other two regions examined are secondary sources that have been suggested to contribute to the ENSO signal in the North Atlantic and Europe. In the Tropical Atlantic (Fig. 4c), the models systematically overestimate the response, an issue which is not improved in the EERIE runs. In the Western Atlantic (Fig. 4d), the observed value is again well within the range of the simulations, and the EERIE models display an average performance comparable to HighResMIP, with the only surprise of IFS-NEMO, which is the second-best model (see ranking details in Fig. 10, 6th column).

https://doi.org/10.5194/egusphere-2026-547
Preprint. Discussion started: 11 February 2026

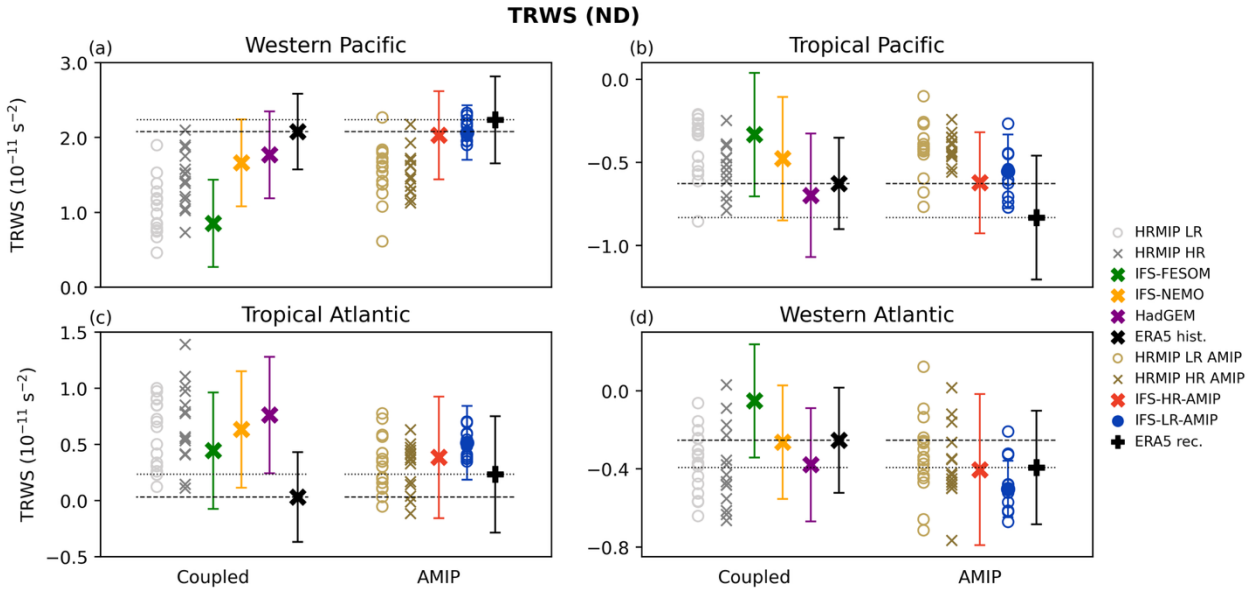

Figure 4: Linear regression on the N3.4 index of 200-hPa TRWS anomalies averaged over the 4 areas detailed in the text: (a) Western Pacific (b) Tropical Pacific (c) Tropical Atlantic (d) Western Atlantic. In each panel, coupled runs are on the left and AMIP runs are on the right. ERA5 hist. =1950-2014, ERA5 rec.= 1980-2023. The empty blue circles indicate the single members form the EERIE IFS-LR ensemble, with the filled circle represent the ensemble mean. The vertical bars indicate the confidence interval at the 95% level.

3.3 Wave train

The next natural step is to examine how the EERIE models reproduce the extra-tropical response and specifically the Rossby wave train, which emerges clearly in the 200-hPa geopotential height (Fig. 5). Due to the different nature of the early-winter and late-winter responses, we consider the two seasons separately and define distinct diagnostics to assess them.

3.3.1 Early winter (ND)

In early winter, the Rossby wave train is not established yet in reanalysis: only weak cyclonic anomalies are present in the North Pacific, while a dipole with negative anomalies at high latitudes and positive ones at mid latitudes dominates the North Atlantic (Fig. 5a). The EERIE models broadly capture the response in the North Pacific, though IFS-FESOM seems to anticipate a JF-like response (Fig.5b), while HadGEM simulates a low pressure that is excessively shifted to the east (Fig. 5d). Note, however, that this response in the North Pacific is not significant in IFS-NEMO and only partially in ERA5 (Fig. 5a,c). Since the center of action in the North Pacific is not fully formed, we evaluate the models' performance with a simple average over the area 180-120°W, 30-60°N (green box in Fig.5). According to this metric (Fig. 6a), IFS-NEMO and HadGEM show

https://doi.org/10.5194/egusphere-2026-547
Preprint. Discussion started: 11 February 2026

an average performance (ranking n. 11 and 12, respectively), while IFS-FESOM is among the worst models (n. 27), though still within the range of HighResMIP, which is rather large (Fig. 6a).

In the North Atlantic, given the dipolar pattern, we evaluate the response based on the difference between the two boxes at 70°W-0°, 50-70°N and 70°W-0, 30-50°N (displayed in Fig. 5), which is expected to be negative in this season. Despite the large spread, all models systematically underestimate the amplitude and sometimes produce an opposite-signed response (Fig. 6c; note the different scales in panels a,c, and d). IFS-NEMO and HadGEM score well in this metric, ranking n. 6 and 12, respectively (Fig. 6c); however, the spatial patterns are rather different and not significant at mid latitudes (Fig. 5b,c). In contrast, IFS-FESOM is again one of the worst performers when it comes to this early-winter response (n. 27; Fig. 6d).

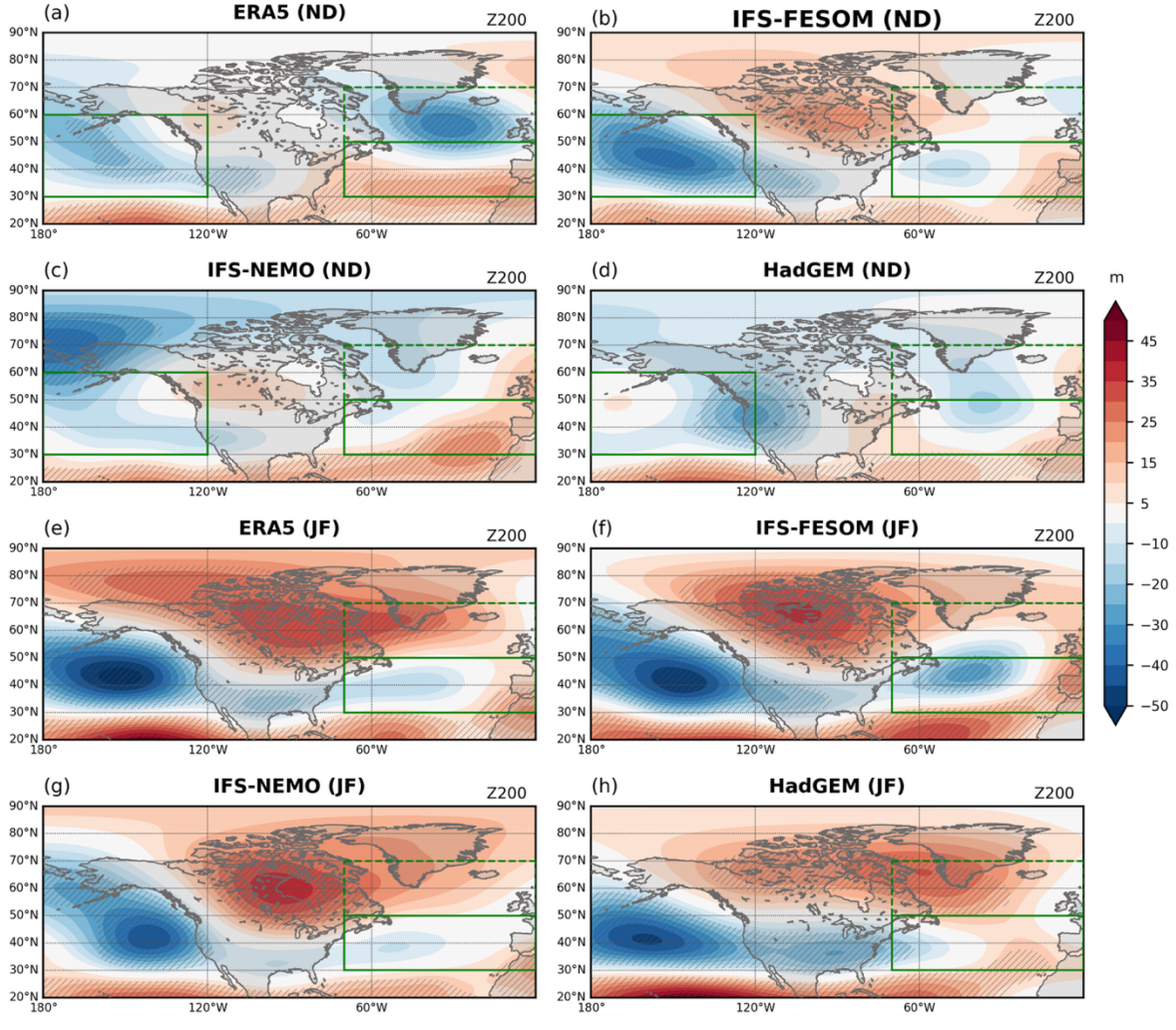

Figure 5: Linear regression on the N3.4 index of 200-hPa geopotential height anomalies in (a-d) Nov-Dec and (e-h) Jan-Feb, for ERA5 and the EERIE coupled models. Hatches indicate statistical significance at the 95% level. The green boxes show the regions used to compute the averages shown in Figs. 6 and 7.

https://doi.org/10.5194/egusphere-2026-547
Preprint. Discussion started: 11 February 2026

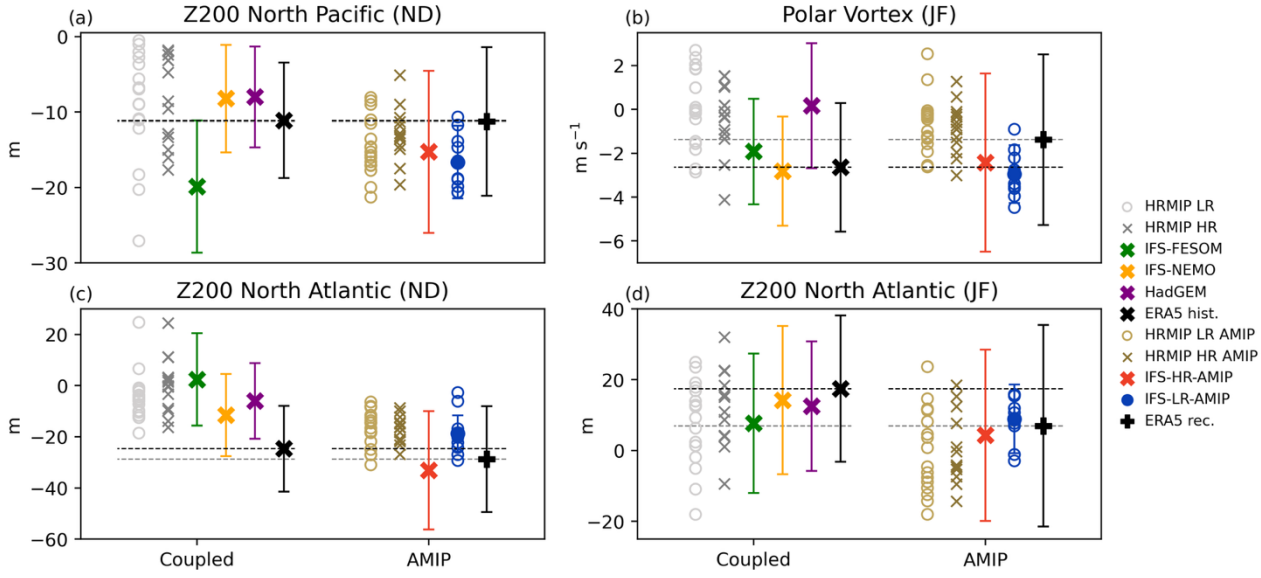

Figure 6: Linear regression on the N3.4 index of (a) 200-hPa geopotential height averaged over the North Pacific box shown in Fig. 6 in Nov-Dec (b)10-hPa zonal-mean zonal wind at 60°N in Jan-Feb (c,d) 200-hPa geopotential height dipole in the North Atlantic, as described in the main text, in Nov-Dec and Jan-Feb. In each panel, coupled runs are on the left and AMIP runs are on the right. ERA5 hist. =1950-2014, ERA5 rec.= 1980-2023. The empty blue circles indicate the single members form the EERIE IFS-LR ensemble, with the filled circle represent the ensemble mean. The vertical bars indicate the confidence interval at the 95% level.

3.3.2 Late winter (JF)

The wave train is fully developed in late winter, with distinguished centres of action of alternating sign over the North Pacific, North America and North Atlantic (Fig. 5e). The EERIE models adequately capture the signal in the North Pacific (Fig. 5f-h), which we characterize in a similar manner as we did for the tropical response. After considering the anomalous response in the band 30-50°N (Fig. S4), we locate the minimum and report its longitude and amplitude in a scatterplot (Fig. 7a). The simulated values are roughly centered around ERA5, with the EERIE models well within the HighResMIP range. In this case, the EERIE models perform overall well in terms of amplitude, with all three scoring better than most HighResMIP members (see Fig. 10, 9th column). The case of IFS-FESOM is particularly interesting, since it is one of the most accurate models in capturing the observed amplitude (ranking n.3), despite its deficiencies in the previous steps. Concerning the longitude, they are in the range of HighResMIP, with average performance (Fig. S5).

A similar assessment can be carried out for the anomalous anticyclone at high latitudes, for which we define a corresponding metric using the latitudinal band 50-80°N (Fig. S4). More than half of the members simulate a response that is too weak and shifted to the west, but there is considerable variety and spread (Fig. 7c). Similarly to the North Pacific, the EERIE models show again a good representation of the amplitude, with some of the smallest errors: IFS-FESOM is the best model, IFS-NEMO ranks n. 6 and HadGEM n. 12. In contrast, HadGEM is one of the worst-performing models in terms of longitude: as

https://doi.org/10.5194/egusphere-2026-547
Preprint. Discussion started: 11 February 2026

already evident in the spatial maps (Fig. 5h), the center of action at high latitudes in this model is shifted to the east of more than 30° (Fig. 7c), with only three HighResMIP members with a larger shift (Fig. S5).

The observed late-winter response in the North Atlantic is again a dipole, but with opposite sign and limited statistical significance even in the reanalysis (Fig. 5e). Characterizing the third center of action of the wave train in the mid latitudes by locating its minimum is not straightforward, as it sometimes consists of two peaks (like in ERA and IFS-NEMO, Fig. 5e,g). We thus assess the response with the same metric used for early winter, though it also involves part of the high-latitude response that we have already examined. This metric is expected to change sign from negative to positive between early and late winter, a switch that most HighResMIP members capture, though with a large spread and values often too small compared to ERA5 (Fig. 6d). According to this metric, the EERIE models perform quite well, with both IFS-NEMO and HadGEM in the upper tercile of the ranking (n. 8 and 11, respectively; details in Fig. 10, 11th column). However, we stress that, besides the limited statistical significance, the simulated spatial patterns have varying location and extension of the anomalies (Fig. 5f-h), which then reflect on the surface signal, as discussed in Sec. 3.5.

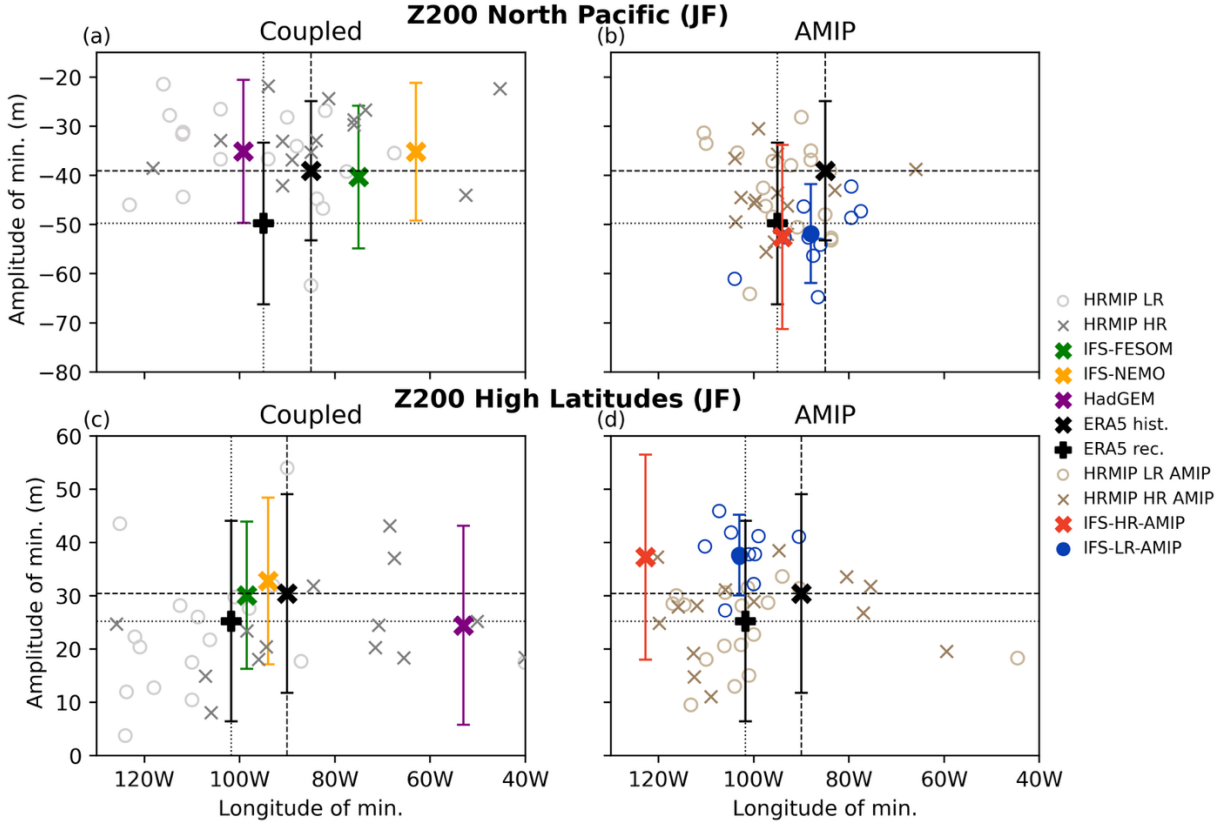

Figure 7: Top: Longitude and amplitude of the minimum in the 200-hPa geopotential height anomalies averaged between 30°N-50°N and regressed on the N3.4 index, in Jan-Feb. Bottom: same, but for the maximum in the band 50°N-80°N. Left: Coupled runs. Right: AMIP runs. ERA5 hist. =1950-2014, ERA5 rec.= 1980-2023. The empty blue circles indicate the single members form the EERIE IFS-LR ensemble, with the filled circle represent the ensemble mean. The vertical bars indicate the confidence interval at the 95% level. In (c), a limit of 40°W has been imposed.

https://doi.org/10.5194/egusphere-2026-547
Preprint. Discussion started: 11 February 2026

3.4 Stratospheric polar vortex

Before examining the surface signals, we first assess the stratospheric response, as this can in turn impact the lower troposphere. The expected deceleration on the polar vortex in late winter emerges clearly in the observed anomalous zonal-mean zonal wind between 50° and 80°N and is captured by IFS-FESOM and IFS-NEMO, but not by HadGEM (Fig. S6). We then use the regression of the zonal-mean zonal wind at 60°N and 10 hPa as a simple metric to encapsulate this response (Fig. 6b). Several HighResMIP members of both high and low resolution produce an opposite-signed response, and those with the correct sign tend to underestimate the deceleration. This is in line with previous studies showing that, while the stratospheric response is a robust feature in ensemble and multi-model means, single members often struggle to simulate it (e.g. Domeisen et al. 2019). The observed response is also largely uncertain, and even though HadGEM's lack of signal is striking, it still falls within the range of uncertainty (and within the HighResMIP range). We also note that extending the analysis to the full period available for HadGEM (1850-2014), the signal becomes consistent with the observational estimate (Fig.S7). In contrast, IFS-FESOM and IFS-NEMO are among the best members over the usual period 1950-2014 (ranking n. 2 and n. 5, respectively), confirming their overall good performance in the late-winter extra-tropical response.

3.5 Surface response in the North Atlantic

Lastly, we examine the ENSO impact on the large-scale surface circulation in the North Atlantic and Europe, which is notoriously a challenging aspect in climate models. The observed early-winter response, a NAO-like SLP dipole with stronger anomalies at high latitudes, is mostly statically significant (Fig. 8a). Observing the corresponding maps, it is evident that the EERIE models do not capture this response and mostly simulate weak, non-significant patterns (Fig. 8b-d). Indeed, the spatial correlation between the EERIE models and ERA5 is around 0.4 for IFS-NEMO and HadGEM, and negative for IFS-FESOM (Fig. 9a). However, this is in line with HighResMIP, whose majority of members also have a correlation that is either negative or weakly positive. Only three members reach around 0.8, but the mean error remains high because of the too low standard deviation. The large inability of the models to capture the early-winter surface signal in the North Atlantic is linked to the poor representation of the wave train (Sect. 3.3), and the similarity between the surface and upper-tropospheric patterns is evident in the EERIE models (cf. Figs. 5b-d and 7b-d).

In late winter, a roughly opposite response is expected, namely a dipole reminiscent of a negative NAO (Fig. 8e). Though this is a well-documented response, note that the high-latitude lobe is only partially significant in the ERA5 sample used here. Additionally, non-significant positive (negative) anomalies over western (eastern) Europe appear, which are known to be less robust signals (e.g. Mezzina et al., 2023). The mid-latitude negative anomaly is present and significant in all the EERIE models (Fig. 8f-h), though it is too prominent in IFS-FESOM, where it dominates the North Atlantic, in agreement with the pattern at upper levels (cf. Figs. 8f,5f). The positive anomaly is not as well captured, as it is mostly too weak and not statistically significant. The HighResMIP models' performance is enhanced compared to early winter, with most members showing a

https://doi.org/10.5194/egusphere-2026-547
Preprint. Discussion started: 11 February 2026

correlation above 0.5, though with varying standard deviations (Fig. 9c). The EERIE models behave similarly, also improving compared to early winter. In line with their good ranking in the late-winter Rossby wave train metric over the North Atlantic, IFS-NEMO and HadGEM are again some of the closest members to ERA5.

385

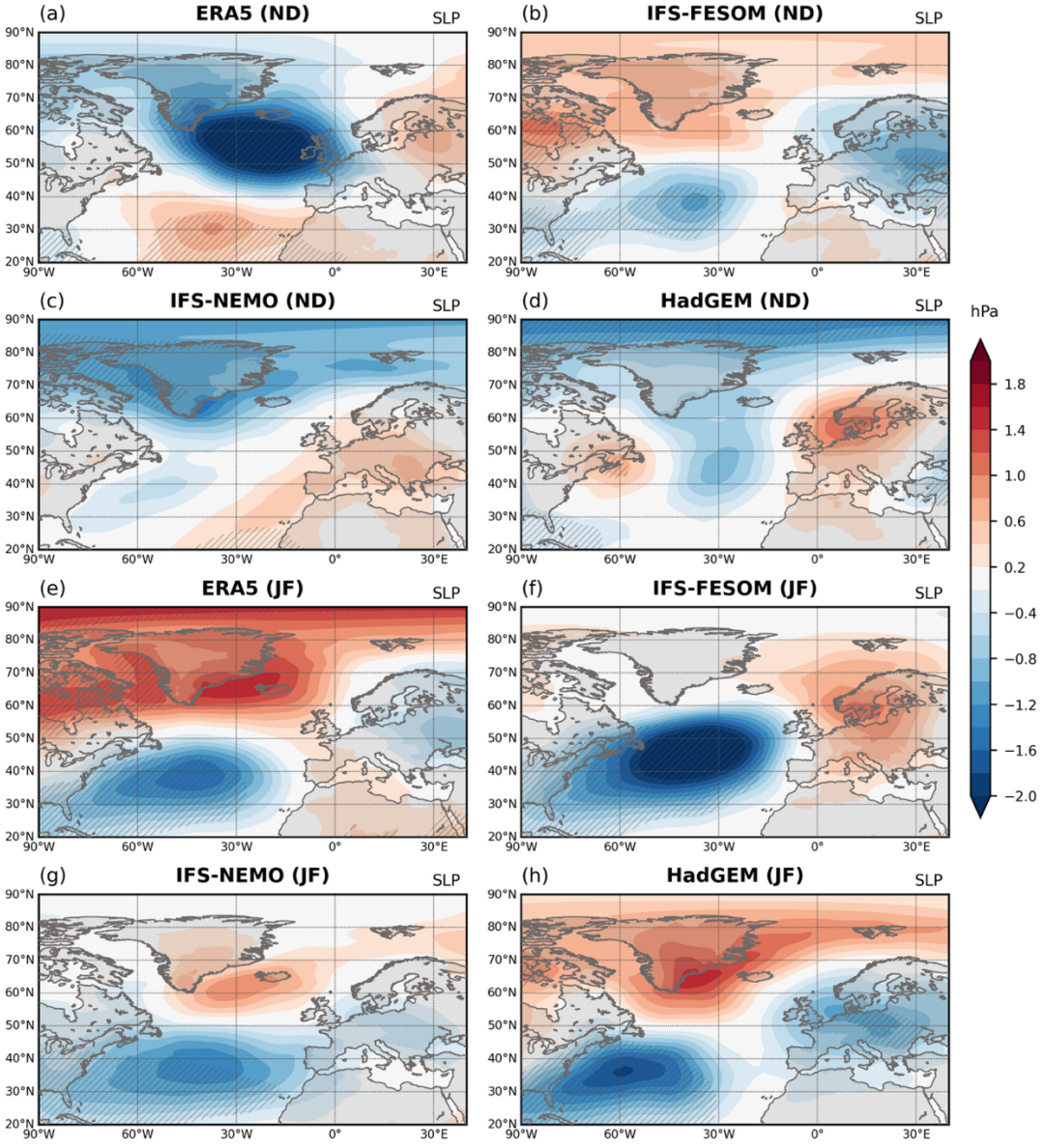

Figure 8: Linear regression on the N3.4 index of SLP anomalies in (a-d) Nov-Dec and (e-h) Jan-Feb, for ERA5 and the EERIE coupled models. Hatches indicate statistical significance at the 95% level. The domain depicted is the one used to build Fig. 9.

https://doi.org/10.5194/egusphere-2026-547
Preprint. Discussion started: 11 February 2026

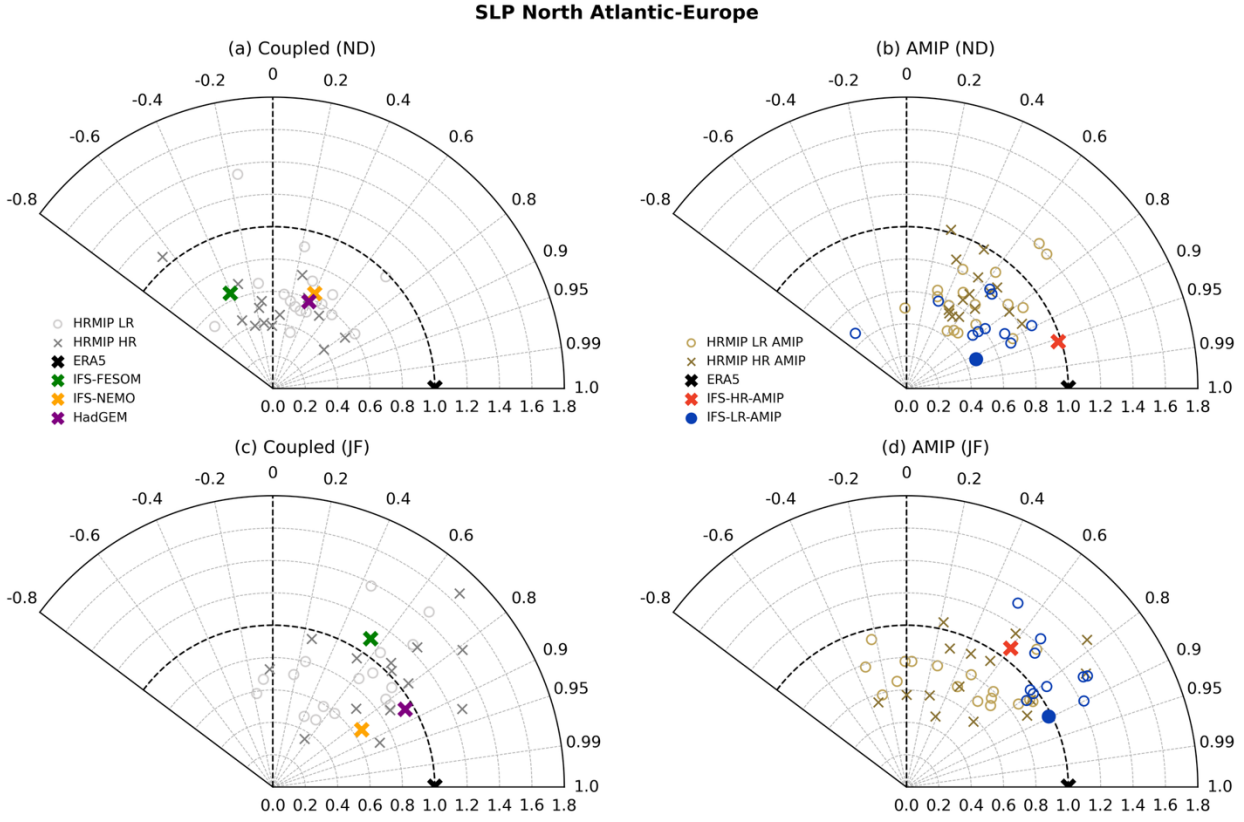

Figure 9: Taylor plots for the anomalous SLP patterns in the NAE sector in (a,b) Nov-Dec and (c,d) Jan-Feb. Left: Coupled runs. Right: AMIP runs. The empty blue circles indicate the single members form the EERIE IFS-LR ensemble, with the filled circle represent the ensemble mean. Note that ERA5-rec (1980-20123) is used as reference pattern for the EERIE AMIP experiments, while ERA5-hist (1950-2014) is used for all the other models. See main text for details on the computation.

4. Results from the atmosphere-only runs

In this section, we examine the set of atmosphere-only simulations run with IFS at two different atmospheric resolutions (see Methods). The objective of this analysis is threefold: first, we can examine how prescribing the SST from observations affects the atmospheric response, also considering that the EERIE AMIP runs, IFS-FESOM and IFS-NEMO share the same atmospheric model. Indeed, the atmospheric teleconnections are intrinsically linked to the representation of ENSO itself, which is often flawed in coupled models. Additionally, other basins can have an influence, like the Indian and Atlantic Oceans, which are also commonly affected by SST biases. Second, we can estimate the impact of increasing the atmospheric resolution only, independent of the ocean. Lastly, the 10 members available for the low-resolution configuration allow us to place the differences between resolutions within the context of internal variability. The EERIE AMIP simulations are compared here with similar SST-forced simulations from HighResMIP (see Methods). Note also that, in this section, HighResMIP is compared with ERA5-hist (1950-2014) and the EERIE runs with ERA-rec (1980-2023), whose values are often different.

https://doi.org/10.5194/egusphere-2026-547
Preprint. Discussion started: 11 February 2026

Concerning the general impact of constraining SST, it is positive on the tropical response, which shows overall a smaller spread and better representation of the amplitude (Fig. 2b,d). IFS in atmosphere-only configuration performs better than its coupled counterparts when compared to the respective observational references (Fig. S8). The prescribed SSTs also act favourably on the early winter signal: the HighResMIP ensembles have reduced spread in both the North Pacific and North Atlantic (cf. grey and brown marks in Fig. 6a,c) and improved amplitudes in the North Atlantic. This is then reflected on the surface signal, where the correlations are enhanced (Fig. 9b). Similarly, improved amplitudes and spread are found in the North Pacific in late winter (Fig. 7b). IFS-HR and most IFS-LR members outperform IFS-FESOM and IFS-NEMO in the North Atlantic in early winter both in the upper troposphere (Fig. S9) and at the surface (Fig. 9), but not so clearly in the North Pacific in either season (Fig. S9, S10).

Interestingly, the prescribed SSTs do not necessarily improve the simulated response in the TRWS (Fig. 4). Although the spread is reduced in most cases, the response is typically too weak in the Pacific (Fig. 4a,b) and too strong in the Atlantic (Fig. 4c,d), though some improvement appears in the SST-forced version of IFS versus the coupled (Fig. S11). There is also no clear benefit from the constrained SST on the late-winter signal in the North Atlantic (Fig. 6d, Fig. S9), at higher latitudes (Fig. 7d, Fig. S10) and in the polar vortex (Fig. 6b, Fig. S9).

When comparing the performance of IFS-HR to the IFS-LR ensemble, it is hard to spot any systematic improvement. In most cases, the high-resolution member is found within the range of the low-resolution ensemble, indicating that any difference could simply arise from internal variability. One exception is the early-winter response in the North Atlantic: at upper-levels (Fig. 6c), IFS-HR (red cross) is slightly outside the IFS-LR range (blue dots), and similarly at surface, where it is the closest member to ERA5 (Fig. 9b). The other case in which the high-resolution member is distinctively outside the low-resolution ensemble is the late-winter response at high latitudes, but for the worse, since it is far too west (Fig. 7d). On the other hand, it is similar in terms of amplitude, since all the EERIE members tend to overestimate it.

https://doi.org/10.5194/egusphere-2026-547
Preprint. Discussion started: 11 February 2026

5. Summary and Discussion

Do eddy-rich models simulate better ENSO teleconnections? This is the question we have been trying to answer by examining three novel coupled systems developed within the EERIE project. According to our diagnostics, which have been designed to encapsulate different aspects of the atmospheric ENSO teleconnections, there is no clear evidence for a systematic improvement with respect to existing, non-eddy-rich simulations run with similar protocol.

Increasing the horizontal resolution in the ocean has been shown to improve known biases in the mean tropical SST and the ENSO tongue, which can in turn positively impact the representation of convection and precipitation associated with ENSO (e.g. Liu B. et al., 2022; Williams et al., 2024). This is not evident in the EERIE coupled models, which do not fully capture the observed tropical response and in fact perform worse than most HighResMIP members (Fig. 10, columns 1 and 2). Other configurations of the EERIE models are known to be affected by biases and errors in this region (e.g. Döscher et al., 2022; Roberts M. et al. 2019), which are likely inherited in this set up, without considerable improvement from the resolution.

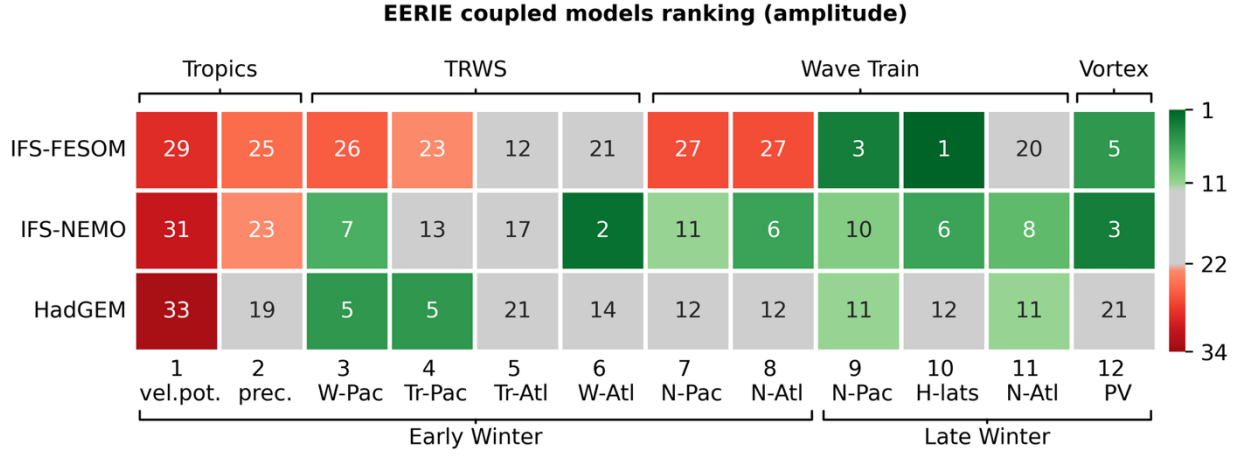

Figure 10: Summary of the ranking for the EERIE models based on the amplitude, for each metric. Columns 1-2: tropical response in the velocity potential and precipitation, see Sect. 3.1. Columns 3-6: TRWS, see Sect. 3.2. Columns 7-11: extra-tropical 200-hPa geopotential height, see Sect. 3.3. Column 12: stratospheric polar vortex, see Sect. 3.4. Red indicates that the EERIE models are worse than most HighResMIP members (lower tercile), green that they are better (upper tercile), grey that they are average.

Though the EERIE models rarely surpass HighResMIP, it is interesting that their relative performance improves in the other metrics linked to the amplitude. Despite the rather poor results in the tropics, they are average or better than HighResMIP in the TRWS (Fig. 10, columns 3-6). An inadequate representation of the tropical upper-level response could thus be mitigated by the interaction with the climatological vorticity. However, this is potentially related to biases in the wind climatology (Fig. S12) and thus a “good” TRWS is not necessarily linked to a realistic representation of all the processes at play.

Further improvement is observed in the extra-tropics in late winter, where the EERIE models are typically in the upper part of the ranking, though not consistently through all the metrics (Fig. 10, columns 9-12). This concerns again only the metrics

https://doi.org/10.5194/egusphere-2026-547
Preprint. Discussion started: 11 February 2026

related to the amplitude, while the location remains challenging (Fig. S5). This improvement further suggests that the adequate simulation of extra-tropical ENSO teleconnections entails more than the tropical response alone. The possible impact of high resolution could act downstream in the teleconnection, for instance by modulating the basic state, the waveguides and thus the wave train propagation (e.g. Dawson et al., 2011; Sabatani et al., 2025), potentially enhancing the representation of late-winter signals.

In contrast, early winter continues to be problematic in the EERIE coupled models: though not worse than HighResMIP (Fig. 10, columns 7-8), they are far from capturing the observed patterns, especially in the North Atlantic. This is a common bias in climate models, whose causes are argued (e.g. Ayarzagüena et al., 2018; Molteni et al., 2020). The mechanisms driving the early-winter ENSO teleconnection to the North Atlantic are still debated in the first place, and other basins like the Indian and Atlantic Ocean have been suggested to contribute to this response (e.g. Abid et al., 2021; Molteni and Brookshaw, 2023). Possible benefits from the increased resolution might be outweighed by biases in these basins, which remain substantial in the EERIE models (Strommen et al. 2025).

Indeed, the atmosphere-only simulations confirm that prescribing the global SSTs improves the representation of the early-winter teleconnection. Instead, the impact is less clear in the TRWS and in the extra-tropics in late winter, supporting the hypothesis that different mechanisms – and basins – are at play in the two seasons. The early-winter surface teleconnection in the North Atlantic is also the only indication of a better performance of the high-resolution member. Apart from that, the AMIP runs do not provide any evidence for a more accurate representation of the ENSO teleconnections in the configuration with increased horizontal resolution in the atmosphere. Nevertheless, we emphasize that a finer atmospheric resolution may be beneficial when further changes are incorporated, such as reducing the use of parameterization schemes (e.g. for convection). This is not the focus of the experiments examined here but is an ongoing effort that will require further investigation (Segura et al., 2025). We also note that the AMIP runs are affected by the limited, identical sample of ENSO events, which could impact the regression estimates.

We acknowledge that our metrics present some limitations. For instance, we have selected the precipitation maximum and velocity potential minimum to encapsulate the tropical response, which indicate a poor performance of the EERIE models. However, we assess the anomalous TRWS on several regions that involve also the large-scale adjustments over the Maritime continent and South America. We also use different methods for different seasons and fields and generally favour simplicity – for instance by using area averages – over precision. More broadly, it is obviously not possible to capture all the mechanisms at play with this restricted number of metrics. Though we consider that these metrics are valid to assess the (lack of) systematic improvement in the EERIE models, other diagnostics are needed to further disentangle the chain of processes, which is beyond our scope.

Finally, our results highlight once again the predominant role of internal variability. This emerged in the 10-member ensemble of AMIP runs, in the limited statistical significance of the spatial patterns in the coupled models, and even in the differences between ERA5-hist and ERA5-rec (though non-stationarity in the teleconnection could also contribute, e.g. Rodriguez-Fonseca et al., 2016). The issue of sampling in assessing ENSO teleconnections is a debated topic (e.g. Deser et al., 2017) and more

https://doi.org/10.5194/egusphere-2026-547
Preprint. Discussion started: 11 February 2026

members from the eddy-rich models would be needed for a more comprehensive assessment: Molteni et al. (2020) suggest at least 5-10 members, which is obviously challenging at these resolutions. Favouring bigger samples is also the rationale for our choice to not distinguish between El Niño and La Niña, though we acknowledge that the impacts from the increased resolution may be more evident in one of the two phases (e.g. Williams et al., 2025).

Within all the limitations detailed above, this first ever assessment of eddy-rich coupled multi-decadal simulations, with ~10 km grid spacing in both ocean and atmosphere, provides mixed results for ENSO teleconnection fidelity compared to previous generation eddy-permitting models. Similarly, atmosphere-only companion experiments also show limited improvements from purely increasing the atmospheric resolution from ~30 to ~10 km.

https://doi.org/10.5194/egusphere-2026-547
Preprint. Discussion started: 11 February 2026

Code and data availability

All EERIE simulation outputs are publicly accessible at https://eerie.cloud.dkrz.de. The Phase 1 simulations used in this study are also available via the Earth System Grid Federation (ESGF; https://esgf-metagrid.cloud.dkrz.de/) and the Centre for Environmental Data Analysis (CEDA) archive (https://archive.ceda.ac.uk/), as explained in Wickramage et al. (2025). The IFS-FESOM outputs are also published in the World Data Center for Climate (Ghosh et al. 2025). The HighResMIP data can be accessed via ESGF and the CEDA archive.

The ERA5 data can be downloaded from the Copernicus Climate Data Store at https://doi.org/10.24381/cds.f17050d7 (single levels) and https://doi.org/10.24381/cds.bd0915c6 (pressure levels).

The velocity potential and TRWS have been computing using the Windspharm Python package (Dawson, 2016).

Author contributions

BM and CR outlined the study. MA, CR, RG, MR and MB contributed to model development, performed the simulations and prepared the data. BM carried out the analyses, prepared the figures and wrote the manuscript with inputs from all co-authors.

Acknowledgements

We sincerely acknowledge Fabian Wachsmann, Chathurika Wickramage and all the EERIE data management team for their work in preparing, storing, maintaining, documenting and providing access to the data. We would also like to acknowledge Marvin Axness and Daria Kuznetsova for their valuable support and contributions to data management.

Financial support

This publication is part of the EERIE project funded by the European Union (Grant Agreement No 101081383). Views and opinions expressed are however those of the authors only and do not necessarily reflect those of the European Union or the European Climate Infrastructure and Environment Executive Agency (CINEA). Neither the European Union nor the granting authority can be held responsible for them. This work was funded by UK Research and Innovation (UKRI) under the UK government's Horizon Europe funding guarantee (grant number 10057890). MR was also supported by the Met Office Hadley Centre Climate Programme funded by DSIT. The production of the IFS–NEMO simulations was supported by the EuroHPC Joint Undertaking through the projects EHPC-EXT-2022E01-007 and EHPC-REG-2025R01-081.

https://doi.org/10.5194/egusphere-2026-547
Preprint. Discussion started: 11 February 2026

References

Abid, M.A., Kucharski, F., Molteni, F., and Almazroui, M.: Predictability of Indian Ocean precipitation and its North Atlantic teleconnections during early winter. npj Clim. Atmos. Sci., 6, 17, https://doi.org/10.1038/s41612-023-00328-z, 2023.

Aengenheyster, M., Roberts, C. D., Aguridan, R., Griffith, M., Hogan, R., Reuter, B., Roberts, M. J., Sarmany, D., Senan, R., Stockdale. T. N., Villaume, S., and Fabian Wachsmann, F.: Multi-decadal high-resolution historical simulations with the ECMWF global atmosphere model. Under review *in Scientific Data*.

Athanasiadis, P. J., Ogawa, F., Omrani, N.-E., Keenlyside, N., Schiemann, R., Baker, A. J., Vidale, P. L., Bellucci, A., Ruggieri, P., Haarsma, R., Roberts, M., Roberts, C., Novak, L., and Gualdi, S.: Mitigating Climate Biases in the Midlatitude North Atlantic by Increasing Model Resolution: SST Gradients and Their Relation to Blocking and the Jet, J. Climate, 35, 3385–3406, https://doi.org/10.1175/JCLI-D-21-0515.1, 2022.

Ayarzagüena, B., Ineson, S., Dunstone, N. J., Baldwin, M. P. and Scaife, A. A.: Intraseasonal Effects of El Niño–Southern Oscillation on North Atlantic Climate, J. Climate, 31, 8861–8873, https://doi.org/10.1175/JCLI-D-18-0097.1, 2018.

Bladé, I., Newman, M., Alexander, M. A., and Scott, J. D.: The late fall extratropical response to ENSO: sensitivity to coupling and convection in the Tropical West Pacific, J. Clim., 21,6101–6118, https://doi.org/10.1175/2008JCLI1612.1, 2008.

Blockley, E., Fiedler, E., Ridley, J., Roberts, L., West, A., Copsey, D., Feltham, D., Graham, T., Livings, D., Rousset, C., Schroeder, D., and Vancoppenolle, M.: The sea ice component of GC5: coupling SI3 to HadGEM3 using conductive fluxes, Geosci. Model Dev., 17, 6799–6817, https://doi.org/10.5194/gmd-17-6799-2024, 2024.

Bryan, F. O., Hecht, M. W., and Smith, R. D.: Resolution convergence and sensitivity studies with North Atlantic circulation models. Part I: The western boundary current system, Ocean Modelling, 16, 141–159, https://doi.org/10.1016/j.ocemod.2006.08.005, 2007.

Dawson, A.: Windspharm: A high-level library for global wind field computations using spherical harmonics, Journal of Open Research Software, 4, e31, https://doi.org/10.5334/jors.129, 2016.

Dawson, A., Matthews, A. J., and Stevens, D. P.: Rossby wave dynamics of the North Pacific extra-tropical response to El Niño: importance of the basic state in coupled GCMs, Clim. Dyn., 37, 391–405, https://doi.org/10.1007/s00382-010-0854-7, 2011.

Dawson, A., Matthews, A. J., Stevens, D. P., Roberts, M. J., and Vidale, P. L.: Importance of oceanic resolution and mean state on the extra-tropical response to El Niño in a matrix of coupled models, Clim. Dyn., 41, 1439–1452, https://doi.org/10.1007/s00382-012-1518-6, 2013.

Deser, C., Simpson, I. R., McKinnon, K. A., and Phillips, A. S.: The Northern Hemisphere extratropical atmospheric circulation response to ENSO: How well do we know it and how do we evaluate models accordingly?, J. Climate, 30, 5059–5082, https://doi.org/10.1175/JCLI-D-16-0844., 2017.

Domeisen, D. I., Garfinkel, C. I., and Butler, A. H.: The teleconnection of El Niño Southern Oscillation to the stratosphere, Rev. Geophys., 57, 5–47, https://doi.org/10.1029/2018RG000596, 2019.

Docquier, D., Grist, J. P., Roberts, M. J., Roberts, C. D., Semmler, T., Ponsoni, L., Massonnet, F., Sidorenko, D., Sein, D. V., Iovino, D., Bellucci, A., and Fichefet, T.: Impact of model resolution on Arctic sea ice and North Atlantic Ocean heat transport, Clim. Dynam., 53, 4989–5017, https://doi.org/10.1007/s00382-019-04840-y, 2019.

https://doi.org/10.5194/egusphere-2026-547
Preprint. Discussion started: 11 February 2026

Dong, C., You, Z., Dong, J., Ji, J., Sun, W., Xu, G., Lu, X., Xie, H., Teng, F., Liu, Y., Xu, A., Wang, Q., Xia, Q., Lin, X., Fu, M., Wang, J., Cao, Y., and Han, G.: Oceanic mesoscale eddies, Ocean-Land-Atmos. Res., 4, 0081, https://doi.org/10.34133/olar.0081, 2025.

Döscher, R., Acosta, M., Alessandri, A., Anthoni, P., Arsouze, T., Bergman, T., Bernardello, R., Boussetta, S., Caron, L.-P., Carver, G., Castrillo, M., Catalano, F., Cvijanovic, I., Davini, P., Dekker, E., Doblas-Reyes, F. J., Docquier, D., Echevarria, P., Fladrich, U., Fuentes-Franco, R., Gröger, M., v. Hardenberg, J., Hieronymus, J., Karami, M. P., Keskinen, J.-P., Koenigk, T., Makkonen, R., Massonnet, F., Ménégoz, M., Miller, P. A., Moreno-Chamarro, E., Nieradzik, L., van Noije, T., Nolan, P., O'Donnell, D., Ollinaho, P., van den Oord, G., Ortega, P., Prims, O. T., Ramos, A., Reerink, T., Rousset, C., Ruprich-Robert, Y., Le Sager, P., Schmith, T., Schrödner, R., Serva, F., Sicardi, V., Sloth Madsen, M., Smith, B., Tian, T., Tourigny, E., Uotila, P., Vancoppenolle, M., Wang, S., Wårlind, D., Willén, U., Wyser, K., Yang, S., Yepes-Arbós, X., and Zhang, Q.: The EC-Earth3 Earth system model for the Coupled Model Intercomparison Project 6, Geosci. Model Dev., 15, 2973–3020, https://doi.org/10.5194/gmd-15-2973-2022, 2022.

Fang, Y., Screen, J. A., Hu, X., Lin, S., Williams, N. C., and Yang, S.: CMIP6 models underestimate ENSO teleconnections in the Southern Hemisphere. Geophys. Res. Lett., 51, e2024GL110738. https://doi.org/10.1029/2024GL110738, 2024.

García-Serrano, J., Cassou, C., Douville, H., Giannini, A., Doblas-Reyes, F. J.: Revisiting the ENSO teleconnection to the tropical North Atlantic, J. Clim, 30,6945–6957, https://doi.org/10.1175/JCLI-D-16-0641.1, 2017

Ghosh, R., Cheedela, S. K., Wickramage, C., Wachsmann, F., Beyer, S., Aengenheyster, M., Becker, T., Rackow, T., Koldunov, N., Sidorenko, D., and Jung, T.: EERIE: Ocean Eddy-rich Kilometer-scale Climate Simulation with Integrated Forecasting System (IFS) – Finite volumE Sea Ice–Ocean Model (FESOM2.5): historical simulation, v1, World Data Center for Climate (WDCC) at DKRZ, https://doi.org/10.26050/WDCC/EERIE_FESOM_hist_v1, 2025.

Guiavarc'h, C., Storkey, D., Blaker, A. T., Blockley, E., Megann, A., Hewitt, H., Bell, M. J., Calvert, D., Copsey, D., Sinha, B., Moreton, S., Mathiot, P., and An, B.: GOSI9: UK Global Ocean and Sea Ice configurations, Geosci. Model Dev., 18, 377–403, https://doi.org/10.5194/gmd-18-377-2025, 2025.

Haarsma, R. J., Roberts, M. J., Vidale, P. L., Senior, C. A., Bellucci, A., Bao, Q., Chang, P., Corti, S., Fučkar, N. S., Guemas, V., von Hardenberg, J., Hazeleger, W., Kodama, C., Koenigk, T., Leung, L. R., Lu, J., Luo, J.-J., Mao, J., Mizielinski, M. S., Mizuta, R., Nobre, P., Satoh, M., Scoccimarro, E., Semmler, T., Small, J., and von Storch, J.-S.: High Resolution Model Intercomparison Project (HighResMIP v1.0) for CMIP6, Geosci. Model Dev., 9, 4185–4208, https://doi.org/10.5194/gmd-9-4185-2016, 2016.

Hallberg, R.: Using a resolution function to regulate parameterizations of oceanic mesoscale eddy effects, Ocean Modelling, 72, 92–103, https://doi.org/10.1016/j.ocemod.2013.08.007, 2013.

Hardiman, S. C., Dunstone, N. J., Scaife, A. A., Smith, D. M., Ineson, S., Lim, J., and Fereday, D.: The impact of strong El Niño and La Niña events on the North Atlantic, Geophys. Res. Lett., 46, 2874–2883, https://doi.org/10.1029/2018GL081776, 2019.

Hersbach, H., Bell, B., Berrisford, P., Hirahara, S., Horányi, A., Muñoz-Sabater, J., Nicolas, J., Peubey, C., Radu, R., Schepers, D., Simmons, A., Soci, C., Abdalla, S., Abellan, X., Balsamo, G., Bechtold, P., Biavati, G., Bidlot, J., Bonavita, M., De Chiara, G., Dahlgren, P., Dee, D., Diamantakis, M., Dragani, R., Flemming, J., Forbes, R., Fuentes, M., Geer, A., Haimberger, L., Healy, S., Hogan, R. J., Hólm, E., Janisková, M., Keeley, S., Laloyaux, P., Lopez, P., Lupu, C., Radnoti, G., De Rosnay, P., Rozum, I., Vamborg, F., Villaume, S., and Thépaut, J. N.: The ERA5 global reanalysis, Q. J. Roy. Meteor. Soc., 146, 1999–2049, https://doi.org/10.1002/qj.3803, 2020.

Hewitt, H. T., Roberts, M., Mathiot, P., Biastoch, A., Blockley, E., Chassignet, E. P., Fox-Kemper, B., Hyder, P., Marshall, D. P., Popova, E., Tréguier, A.-M., Zanna, L., Yool, A., Yu, Y., Beadling, R., Bell, M., Kuhlbrodt, T., Arsouze, T., Bellucci, A., Castruccio, F., Gan, B., Putrasahan, D., Roberts, C. D., Van Roekel, L., and Zhang, Q.: Resolving and parameterising the ocean mesoscale in Earth system models, Curr. Clim. Change Rep., 6, 137–152, https://doi.org/10.1007/s40641-020-00164-w, 2020.

https://doi.org/10.5194/egusphere-2026-547
Preprint. Discussion started: 11 February 2026

Johnson, S. J., Stockdale, T. N., Ferranti, L., Balmaseda, M. A., Molteni, F., Magnusson, L., Tietsche, S., Decremer, D., Weisheimer, A., Balsamo, G., Keeley, S. P. E., Mogensen, K., Zuo, H., and Monge-Sanz, B. M.: SEAS5: the new ECMWF seasonal forecast system, Geosci. Model Dev., 12, 1087–1117, https://doi.org/10.5194/gmd-12-1087-2019, 2019.

Liu, B., Gan, B., Cai, W., Wu, L., Geng, T., Wang, H., Wang, S., Jing, Z., Jia, F.: Will increasing climate model resolution be beneficial for ENSO simulation? Geophysical Research Letters, 49, e2021GL096932, https://doi.org/10.1029/2021GL096932, 2022.

Liu, X., Ma, X., Chang, P., Jia, Y., Fu, D., Xu, G., Wu, L., Saravanan, R., and Patricola, C. M.: Ocean fronts and eddies force atmospheric rivers and heavy precipitation in western North America, Nat. Commun., 12, 1268, https://doi.org/10.1038/s41467-021-21504-w, 2021.

Lock, A. P., Whitall, M., Stirling, A. J., Williams, K. D., Lavender, S. L., Morcrette, C., Matsubayashi, K., Field, P. R., Martin, G., Willett, M., and Heming, J.: The performance of the CoMorph-A convection package in global simulations with the Met Office Unified Model, Q. J. Roy. Meteorol. Soc., 150, 3527–3543, https://doi.org/10.1002/qj.4781, 2024.

Madec, G., Bourdallé-Badie, R., Chanut, J., Clementi, E., Coward, A., Ethé, C., Iovino, D., Lea, D., Lévy, C., Lovato, T., Martin, N., Masson, S., Mocavero, S., Rousset, C., Storkey, D., Müeller, S., Nurser, G., Bell, M., Samson, G., Mathiot, P., Mele, F., and Moulin, A.: NEMO ocean engine, Sci. Notes IPSL Clim. Model. Cent., 27, https://doi.org/10.5281/zenodo.6334656, 2022.

Mezzina, B., J. García-Serrano, I. Bladé, and F. Kucharski, 2020: Dynamics of the ENSO Teleconnection and NAO Variability in the North Atlantic–European Late Winter, J. Clim., 33, 907–923, https://doi.org/10.1175/JCLI-D-19-0192.1, 2020.

Mezzina, B., García-Serrano, J., Bladé, I , Palmeiro, F. M., Batté, L., Ardilouze, C., Benassi, M., and Gualdi, S.: Multi-model assessment of the late-winter extra-tropical response to El Niño and La Niña, Clim. Dyn., 58, 1965–1986, https://doi.org/10.1007/s00382-020-05415-y, 2022.

Mezzina, B., García-Serrano, J., Ambrizzi, T., Matei, D., Manzini, E., and Bladé, I.: Tropospheric pathways of the late-winter ENSO teleconnection to Europe, Clim Dyn 60, 3307–3317, https://doi.org/10.1007/s00382-022-06508-6, 2023.

Molteni, F., and Brookshaw, A.: Early- and late-winter ENSO teleconnections to the Euro-Atlantic region in state-of-the-art seasonal forecasting systems, Clim. Dyn., 61, 2673–2692, https://doi.org/10.1007/s00382-023-06698-7, 2023.

Molteni, F., Roberts, C. D., Senan, R., Keeley, S. P. E., Bellucci, A., Corti, S., Fuentes Franco, R., Haarsma, R., Levine, X., Putrasahan, D., Roberts, M. J., and Terray, L.: Boreal-winter teleconnections with tropical Indo-Pacific rainfall in HighResMIP historical simulations from the PRIMAVERA project, Clim. Dyn., 55, 1843–1873, https://doi.org/10.1007/s00382-020-05358-4, 2020.

Qin, J., and Robinson, W. A.: On the Rossby wave source and the steady linear response to tropical forcing, J. Atmos. Sci., 50,1819–1823, https://doi.org/10.1175/1520-0469(1993)050<1819:OTRWSA>2.0.CO;2, 1993.

Rackow, T., Danilov, S., Goessling, H. F., Hellmer, H. H., Sein, D. V., Semmler, T., Sidorenko, D., and Jung, T.: Delayed Antarctic sea-ice decline in high-resolution climate change simulations, Nat. Commun., 13, 637, https://doi.org/10.1038/s41467-022-28259-y, 2022.

Rackow, T., Pedruzo-Bagazgoitia, X., Becker, T., Milinski, S., Sandu, I., Aguridan, R., Bechtold, P., Beyer, S., Bidlot, J., Boussetta, S., Deconinck, W., Diamantakis, M., Dueben, P., Dutra, E., Forbes, R., Ghosh, R., Goessling, H. F., Hadade, I., Hegewald, J., Jung, T., Keeley, S., Kluft, L., Koldunov, N., Koldunov, A., Kölling, T., Kousal, J., Kühnlein, C., Maciel, P., Mogensen, K., Quintino, T., Polichtchouk, I., Reuter, B., Sármány, D., Scholz, P., Sidorenko, D., Streffing, J., Sützl, B., Takasuka, D., Tietsche, S., Valentini, M., Vannière, B., Wedi, N., Zampieri, L., and Ziemen, F.: Multi-year simulations at kilometre scale with the Integrated Forecasting System coupled to FESOM2.5 and NEMOv3.4, Geosci. Model Dev., 18, 33–69, https://doi.org/10.5194/gmd-18-33-2025, 2025.Roberts, C. D., Senan, R., Molteni, F., Boussetta, S., Mayer, M., and Keeley, S. P. E.: Climate model configurations of the ECMWF Integrated Forecasting System (ECMWF-IFS cycle 43r1) for HighResMIP, Geosci. Model Dev., 11, 3681–3712, https://doi.org/10.5194/gmd-11-3681-2018, 2018.

https://doi.org/10.5194/egusphere-2026-547
Preprint. Discussion started: 11 February 2026

Roberts, C. D., Senan, R., Molteni, F., Boussetta, S., Mayer, M., and Keeley, S. P. E.: Climate model configurations of the ECMWF Integrated Forecasting System (ECMWF-IFS cycle 43r1) for HighResMIP, Geosci. Model Dev., 11, 3681–3712, https://doi.org/10.5194/gmd-11-3681-2018, 2018.

Roberts, M. J., Baker, A., Blockley, E. W., Calvert, D., Coward, A., Hewitt, H. T., Jackson, L. C., Kuhlbrodt, T., Mathiot, P., Roberts, C. D., Schiemann, R., Seddon, J., Vannière, B., and Vidale, P. L.: Description of the resolution hierarchy of the global coupled HadGEM3-GC3.1 model as used in CMIP6 HighResMIP experiments, Geosci. Model Dev., 12, 4999–5028, https://doi.org/10.5194/gmd-12-4999-2019, 2019.

Roberts, M. J., Jung, T., Ortega, P., Ghosh, R., Wachsmann, F., von Storch, J.-S., Kroeger, J., Aengenheyster, M., and Roberts, C. D.: Phase 1 simulations, including HighResMIP and CMIP6- PI-control simulations. Zenodo. https://doi.org/10.5281/zenodo.14288726, 2024.

Roberts, M. J., Vidale, P. L., Senior, C., Hewitt, H. T., Bates, C., Berthou, S., Chang, P., Christensen, H. M., Danilov, S., Demory, M.-E., Griffies, S. M., Haarsma, R., Jung, T., Martin, G., Minobe, S., Ringler, T., Satoh, M., Schiemann, R., Scoccimarro, E., Stephens, G., and Wehner, M. F.: The benefits of global high resolution for climate simulation: process understanding and the enabling of stakeholder decisions at the regional scale, Bull. Amer. Meteorol. Soc., 99, 2341–2359, https://doi.org/10.1175/BAMS-D-15-00320.1, 2018.

Rodríguez-Fonseca, B., Suárez-Moreno, R., Ayarzagüena, B., López-Parages, J., Gómara, I., Villamayor, J., Mohino, E., Losada, T., & Castaño-Tierno, A.: A Review of ENSO Influence on the North Atlantic. A Non-Stationary Signal, Atmos., 7, 87, https://doi.org/10.3390/atmos7070087, 2016.

Sabatani, D., Gualdi, S.: ENSO teleconnections with the NAE sector during December in CMIP5/CMIP6 models: impacts of the atmospheric mean state, npj Clim. Atmos. Sci., 8, 226, https://doi.org/10.1038/s41612-025-01064-2, 2025.

Sardeshmukh, P. D., Hoskins, B. J.: The generation of global rotational flow by steady idealized tropical divergence, J. Atmos. Sci., 45,1228–1251, https://doi.org/10.1175/1520-0469(1988)045<1228:TGOGRF>2.0.CO;2, 1988.

Segura, H., Pedruzo-Bagazgoitia, X., Weiss, P., Müller, S. K., Rackow, T., Lee, J., Dolores-Tesillos, E., Benedict, I., Aengenheyster, M., Aguridan, R., Arduini, G., Baker, A. J., Bao, J., Bastin, S., Baulenas, E., Becker, T., Beyer, S., Bockelmann, H., Brüggemann, N., Brunner, L., Cheedela, S. K., Das, S., Denissen, J., Dragaud, I., Dziekan, P., Ekblom, M., Engels, J. F., Esch, M., Forbes, R., Frauen, C., Freischem, L., García-Maroto, D., Geier, P., Gierz, P., González-Cervera, Á., Grayson, K., Griffith, M., Gutjahr, O., Haak, H., Hadade, I., Haslehner, K., ul Hasson, S., Hegewald, J., Kluft, L., Koldunov, A., Koldunov, N., Kölling, T., Koseki, S., Kosukhin, S., Kousal, J., Kuma, P., Kumar, A. U., Li, R., Maury, N., Meindl, M., Milinski, S., Mogensen, K., Niraula, B., Nowak, J., Praturi, D. S., Proske, U., Putrasahan, D., Redler, R., Santuy, D., Sármány, D., Schnur, R., Scholz, P., Sidorenko, D., Spät, D., Sützl, B., Takasuka, D., Tompkins, A., Uribe, A., Valentini, M., Veerman, M., Voigt, A., Warnau, S., Wachsmann, F., Wacławczyk, M., Wedi, N., Wieners, K.-H., Wille, J., Winkler, M., Wu, Y., Ziemen, F., Zimmermann, J., Bender, F. A.-M., Bojovic, D., Bony, S., Bordoni, S., Brehmer, P., Dengler, M., Dutra, E., Faye, S., Fischer, E., van Heerwaarden, C., Hohenegger, C., Järvinen, H., Jochum, M., Jung, T., Jungclaus, J. H., Keenlyside, N. S., Klocke, D., Konow, H., Klose, M., Malinowski, S., Martius, O., Mauritsen, T., Mellado, J. P., Mieslinger, T., Mohino, E., Pawłowska, H., Peters-von Gehlen, K., Sarré, A., Sobhani, P., Stier, P., Tuppi, L., Vidale, P. L., Sandu, I., and Stevens, B.: nextGEMS: entering the era of kilometer-scale Earth system modeling, Geosci. Model Dev., 18, 7735–7761, https://doi.org/10.5194/gmd-18-7735-2025, 2025.

Strommen, K., Roberts, C., Aengenheyster, M., Mezzina, B., and Dey, I: Impact of the ocean mesoscale on the atmospheric mean state. Zenodo. https://doi.org/10.5281/zenodo.17951345, 2025.

Taschetto, A. S., Ummenhofer, C. C., Stuecker, M. F., Dommenget, D., Ashok, K., Rodrigues, R. R., and Yeh, S.-W.: ENSO atmospheric teleconnections, in: El Niño Southern Oscillation in a Changing Climate, edited by: McPhaden, M. J., Santoso, A., and Cai, W., https://doi.org/10.1002/9781119548164.ch14, 2020.

Taylor, K. E.: Summarizing multiple aspects of model performance in a single diagram, J. Geophys. Res., 106, 7183–7192, doi:10.1029/2000JD900719, 2001.

https://doi.org/10.5194/egusphere-2026-547
Preprint. Discussion started: 11 February 2026

Toniazzo, T., Scaife, A. A.: The influence of ENSO on winter North Atlantic climate, Geophys. Res. Lett., 33, L24704, https://doi.org/10.1029/2006GL027881, 2006.

Trenberth, K. E., Branstator, G. W., Karoly, D., Kumar, A., Lau, N.-C., and Ropelewski, C.: Progress during TOGA in understanding and modeling global teleconnections associated with tropical sea surface temperatures, J. Geophys. Res., 103, 14291–14324, https://doi.org/10.1029/97JC01444, 1998.

Vancoppenolle, M., Rousset, C., Blockley, E., Aksenov, Y., Feltham, D., Fichefet, T., Garric, G., Guémas, V., Iovino, D., Keeley, S., Madec, G., Massonnet, F., Ridley, J., Schroeder, D., and Tietsche, S.: The NEMO Sea Ice Engine (version 4.2, release doc 1.0), Zenodo , https://doi.org/10.5281/zenodo.7534900, 2023.

Wickramage, C., Wachsmann, F., Roberts, M., Iwi, A., Axness Ferrando, M., and Bretonnière, P.-A.: Publication of EERIE Phase 1 Simulations (2.0). Zenodo. https://doi.org/10.5281/zenodo.17465311, 2025.

Williams, N. C., Scaife, A. A., and Screen, J. A.: Effect of increased ocean resolution on model errors in El Niño–Southern Oscillation and its teleconnections, Q. J. Roy. Meteorol. Soc., 150, 1489–1500, https://doi.org/10.1002/qj.4655, 2024.

Yeager, S. G., Chang, P., Danabasoglu, G., Rosenbloom, N., Zhang, Q., Castruccio, F. S., Gopal, A., Cameron Rencurrel, M., and Simpson, I. R.: Reduced Southern Ocean warming enhances global skill and signal-to-noise in an eddy-resolving decadal prediction system, Npj Clim. Atmos. Sci., 6, 107, https://doi.org/10.1038/s41612-023-00434-y, 2023.